Transient Combined Conduction and Radiation with Anisotropic Scattering

Jen-Hui Tsai* and Jenn-Der Lin†
National Chiao Tung University, Hsinchu, Taiwan, Republic of China

The analysis of transient combined radiation and conduction heat transfer in an absorbing, emitting, and anisotropically scattering planar material is investigated theoretically. The medium boundaries are assumed with specified temperatures. Both specular and diffuse reflectivities are included. The Crank-Nicolson method is used to solve the transient energy equation, and the nodal approximation provides the solution for coupled radiative transfer. This solution method may be described as a finite-difference/nodal approximation method and would replace the governing energy and radiative transfer equations by a set of algebraic equations. Using the method, the present study examines the effect of scattering anisotropy on combined conduction and radiation heat transfer. Results are presented for temperature and heat-flux distributions, and results for isotropic scattering are compared to existing data. The agreement is excellent.

Nomenclature

A_1 = linear scattering coefficient
i = dimensionless radiative intensity, $\pi I/(n^2\sigma T_1^4)$
i', i'' = dimensionless boundary intensities
I = radiative intensity
k = thermal conductivity
n = refractive index
N = conduction-radiation parameter, $K\beta/(4n^2\sigma T_1^3)$
p = phase function
q^r = radiative heat transfer
Q^r = dimensionless radiative heat flux, $q^r/(n^2\sigma T_1^4/\pi)$
Q^t = total heat flux
S = source function
T = temperature
β = extinction coefficient
ϵ = surface emissivity
θ = dimensionless temperature (T/T_1) or polar angle
μ = $\cos\theta$
ξ = dimensionless time, $(K\beta^2 t)/\rho C_p$
ρ^d, ρ^s = diffuse and specular reflectivity components, respectively
σ = Stefan-Boltzmann constant
τ = optical distance
ω = scattering albedo

Introduction

In recent years, much research has been conducted on the analysis of steady[1-9] or unsteady[10-18] simultaneous radiation and conduction in an absorbing, emitting, and scattering medium. Some engineering applications of such energy transport analyses are in porous materials, powders and/or fibrous insulations as well as many semitransparent materials. Most of the previously published investigations on transient problems considered isotropic scattering within the medium. However, it is well known that scattering of thermal radiation by real particles, fibers, or impurities in a medium is by no means isotropic and that the anisotropic scattering can play a significant role on overall heat transfer. Tong et al.[17] analyzed transient radiation heat transfer through planar porous materials. They considered semi-isotropic scattering using a two-flux model. Rish and Roux[18] performed an analysis of coupled transient conduction and radiative heat transfer with anisotropic scattering for specularly reflecting boundaries and temperature boundary conditions.

The present work is concerned with anisotropically scattering gray materials, and transient combined conduction and radiation in an absorbing, emitting, and scattering slab with boundaries having specular and diffuse reflectivities is considered. The major difficulty in analysis of such a problem stems from the nonlinear integral differential characteristics of thermal radiation transfer. The present study utilizes the nodal approximation technique, which has been applied successfully in pure radiation problems,[19] to account for the radiation contribution. The energy equation is solved for temperature distribution using the Crank-Nicolson difference technique.

Since the scattering of radiation in many engineering applications can lead to significant anisotropy, the present work first examines the effects of scattering anisotropy on transient temperature and radiative heat-flux distributions during interaction between conduction and radiation in a planar medium, which were not analyzed in Ref. 18. The work also investigates the effect of radiation parameters, such as albedo, surface emissivity, and conduction-to-radiation parameter, on the temperature and radiative heat-flux distributions. Results indicate that the scattering anisotropy has an important effect on the radiative heat flux and total heat flux. In some instances, the difference in results between the anisotropic and isotropic scattering is quite considerable.

Formulation

We consider an absorbing, emitting, and anisotropically scattering planar medium that is initially at a uniform temperature T_0, and for times greater than zero the two boundary surfaces are maintained at specified temperatures of T_1 and T_2, respectively. Both the diffuse and specular reflection components at the boundaries are included. Figure 1 illustrates the physical geometry. For the problem, the transient energy equation reduces to

$$\frac{\partial^2\theta(\tau,\xi)}{\partial\tau^2}-\frac{1}{4\pi N}\frac{\partial Q^r(\tau,\xi)}{\partial\tau}=\frac{\partial\theta(\tau,\xi)}{\partial\xi}, \qquad \text{in } 0<\tau<\tau_0 \qquad (1)$$

with the boundary conditions

$$\theta(0,\xi)=1,\ \theta(T_0,\xi)=\theta_2, \text{ and } \theta(\tau,0)=\theta_0 \qquad (2)$$

Received Aug. 26, 1988; revision received Jan. 20, 1989.

*Graduate Student, Department of Mechanical Engineering.
†Professor, Department of Mechanical Engineering; currently Academic Visitor, Department of Chemical Engineering and Chemical Technology, Imperial College, London.

The dimensionless net radiative heat flux $Q^r(\tau,\xi)$ at the optical distance τ for azimuthally independent radiation is related to the radiation intensity $i(\tau,\mu,\xi)$ by

$$Q^r(\tau,\xi) = 2\pi \int_{-1}^{1} i(\tau,\mu,\xi)\ \mu \mathrm{d}\mu \tag{3}$$

The radiation distributions can be obtained by[19]

$$\begin{aligned} S(\tau,\mu,\xi) &= (1-\omega)\theta^4(\tau,\xi) \\ &+ \frac{\omega}{2}\left\{ \int_0^{\tau}\int_0^1 \frac{1}{\mu'} S(\tau',\mu',\xi) \exp[-(\tau-\tau')/\mu']\, p(\mu,\mu')\, \mathrm{d}\mu'\mathrm{d}\tau' \right. \\ &+ \int_{\tau}^{\tau_0}\int_0^1 \frac{1}{\mu'} S(\tau',-\mu',\xi) \exp[-(\tau'-\tau)/\mu']\, p(\mu,-\mu')\mathrm{d}\mu'\mathrm{d}\tau' \\ &+ \int_0^1 i(0,\mu',\xi) \exp(-\tau/\mu']\, p(\mu,\mu')\, \mathrm{d}\mu' \\ &\left. + \int_0^1 i(\tau_0,-\mu',\xi) \exp[-(\tau_0-\tau)/\mu']\, p(\mu,-\mu')\, \mathrm{d}\mu' \right\} \end{aligned} \tag{4}$$

where S is the source function, which is the sum of emitted radiation and in-scattered radiation. $i(0,\mu,\xi)$ and $i(\tau_0,-\mu,\xi)$ are dimensionless boundary intensities given by

$$\begin{aligned} i(0,\mu,\xi) &= \epsilon_1 + 2\rho_1^d \left[\int_0^{\tau_0}\int_0^1 S(\tau',-\mu',\xi) \exp(-\tau'/\mu']\, \mathrm{d}\mu'\mathrm{d}\tau' \right. \\ &\left. + \int_0^1 i(\tau_0,-\mu',\xi) \exp(-\tau_0/\mu')\, \mu'\mathrm{d}\mu' \right] \\ &+ \rho_1^s \left[\int_0^{\tau_0} S(\tau',-\mu',\xi) \exp(-\tau'/\mu'] \frac{\mathrm{d}\tau'}{\mu} \right. \\ &\left. + i(\tau_0,-\mu',\xi) \exp(-\tau_0/\mu' \right] \quad \text{for } \mu>0 \end{aligned} \tag{5}$$

and

$$\begin{aligned} i(\tau_0,-\mu,\xi) &= \epsilon_2\theta_2^4 + 2\rho_2^d \\ &\times \left[\int_0^{\tau_0}\int_0^1 S(\tau',\mu',\xi) \exp[-(\tau_0-\tau')/\mu']\, \mathrm{d}\mu'\mathrm{d}\tau' \right. \\ &\left. + \int_0^1 i(0,\mu,\xi) \exp(-\tau_0/\mu')\, \mu'\mathrm{d}\mu' \right] \\ &+ \rho_2^s \left\{ \int_0^{\tau_0} S(\tau',\mu,\xi) \exp[-(\tau_0-\tau)/\mu] \frac{\mathrm{d}\tau'}{\mu} \right. \\ &\left. + i(0,\mu,\xi) \exp(-\tau_0/\mu \right\} \quad \text{for } \mu>0 \end{aligned} \tag{6}$$

where μ is the cosine of the angle between the direction of the radiation intensity and the τ axis. ϵ_1 and ϵ_2 are the emissivities, ρ_1^d and ρ_2^d the diffuse reflectivities, and ρ_1^s and ρ_2^s the specular reflectivities at the surfaces $\tau = 0$ and $\tau = \tau_0$, respectively. $p(\mu,\mu')$ is the scattering phase function. In the present investigation, both linearly anisotropic scattering and Rayleigh scattering are considered to examine the effect of scattering anisotropy. The linearly anisotropic scattering phase function is expressed as $p(\mu,\mu') = 1 + A_1\mu\mu'$, in which A_1 is constant. $A_1 \to 1$ represents strong forward scattering, whereas $A_1 \to -1$ corresponds to strong backward scattering.

The Rayleigh scattering phase function is expressed as

$$p(\mu,\mu') = 3/8\,[3 - \mu^2 + (3\mu^2 - 1)\mu'^2]$$

This phase function is applicable in all problems of scattering by particles with small size parameters, regardless of their shape.

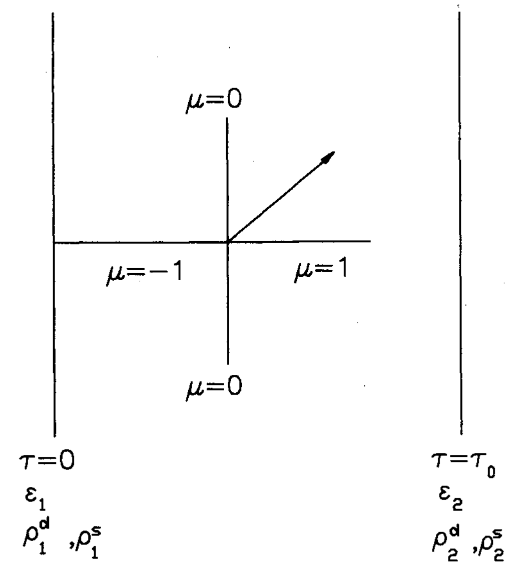

Fig. 1 Physical geometry.

Equations (4-6) formulate the radiative transfer within anisotropically scattering media bounded by plane-parallel surfaces. Radiation distributions may be obtained by first solving the source function and boundary intensities.[20] The net radiative heat flux [Eq. (3)] can be expressed in terms of boundary intensities and the source function as

$$\begin{aligned} Q^r(\tau,\xi) &= \frac{1}{2}\left\{ \int_0^{\tau}\int_0^1 S(\tau',\mu',\xi) \exp[-(\tau-\tau')/\mu']\, p(\mu,\mu')\, \mathrm{d}\mu'\mathrm{d}\tau' \right. \\ &\left. + \int_0^1 i(0,\mu',\xi) \exp(-\tau/\mu')\, \mu'\mathrm{d}\mu' \right\} \\ &- \frac{1}{2}\left\{ \int_{\tau}^{\tau_0}\int_0^1 S(\tau',-\mu',\xi) \exp[-(\tau'-\tau)/\mu']\, \mathrm{d}\mu'\mathrm{d}\tau' \right. \\ &\left. + \int_0^1 i(\tau_0,-\mu',\xi) \exp[-(\tau_0-\tau)/\mu']\, \mu'\mathrm{d}\mu' \right\} \end{aligned} \tag{7}$$

Once the temperature distribution is obtained by using the preceding equations, the total heat flux in the medium is then equal to the sum of both conductive flux and radiative heat flux and can be written as

$$Q^t(\tau,\xi) = \frac{q(\tau,\xi)}{k\beta T_1} = -\frac{\partial\theta(\tau,\xi)}{\partial\tau} + \frac{1}{4\pi N} Q^r(\tau,\xi) \tag{8}$$

Numerical Calculations and Results

Because of the complexity of the radiation nature as well as the nonlinear dependency of radiation emission on temperature, analytic solutions are difficult to obtain. The following solutions are obtained with the radiation contribution solved by nodal approximation technique and the energy equation solved by Crank-Nicolson technique.[21] The current solution method may be described briefly as a finite-difference/nodal approximation scheme. The scheme replaces the original governing energy and radiative transfer equations by a set of algebraic equations; thus, the entire process is, in reality, very efficient.

To perform the numerical calculation of radiation distributions, the whole domain, $0 \le \tau \le \tau_0$ and $-1 \le \mu \le 1$, is subdivided into rectangular subdomains in the τ-μ plane. Let $S_{\mathrm{ap}}(\tau,\mu,\xi)$ be an approximation of $S(\tau,\mu,\xi)$, $i_{\mathrm{ap}}(0,\mu,\xi)$ an approximation of $i(\tau_0,-\mu,\xi)$. If a linear approximation over each subdomain is considered for the source function and

Table 1 Comparison of the transient temperature distribution with isotropic scattering at $\xi = 0.05$, $\tau_0 = 1$, $\theta_1 = 1$, $\theta_2 = 0$, $\theta_0 = 0$, $\omega = 0.5$, and $N = 0.1$ for several wall reflectivity cases

Boundary conditions					Temperature distribution at		
ϵ_1	ρ_1^d	ϵ_2	ρ_2^d	Investigators	$\tau = 0.25$	$\tau = 0.50$	$\tau = 0.75$
1	0	1	0	Lii and Ozisik[12]	0.4617	0.1474	0.0277
1	0	1	0	Sutton[11]	0.4888	0.1778	0.0591
1	0	1	0	Barker and Sutton[10]	0.4893	0.1775	0.0588
1	0	1	0	Present work	0.4889	0.1773	0.0588
1	0	0	1	Lii and Ozisik[12]	0.4716	0.1630	0.0545
1	0	0	1	Sutton[11]	0.5030	0.2005	0.0833
1	0	0	1	Barker and Sutton[10]	0.5035	0.2003	0.0831
1	0	0	1	Present work	0.5031	0.2001	0.0830
0.5	0.5	0.5	0.5	Lii and Ozisik[12]	0.4323	0.1196	0.0195
0.5	0.5	0.5	0.5	Sutton[11]	0.4671	0.1591	0.0499
0.5	0.5	0.5	0.5	Barker and Sutton[10]	0.4675	0.1587	0.0496
0.5	0.5	0.5	0.5	Present work	0.4671	0.1585	0.0495

Table 2 Comparison of the transient net radiative heat-flux distributions with isotropic scattering at $\xi = 0.05$, $\tau_0 = 1$, $\theta_1 = 1$, $\theta_2 = 0$, $\theta_0 = 0$, $\omega = 0.5$, and $N = 0.1$ for several wall reflectivity cases

Boundary conditions					Net radiative heat flux, $Q^r/4\pi N$, at		
ϵ_1	ρ_1^d	ϵ_2	ρ_2^d	Investigators	$\tau = 0.0$	$\tau = 0.5$	$\tau = 1.0$
1	0	1	0	Lii and Ozisik[12]	1.6436	1.2529	0.9746
1	0	1	0	Sutton[11]	1.9304	1.3305	0.8332
1	0	1	0	Barker and Sutton[10]	1.9300	1.3314	0.8335
1	0	1	0	Present work	1.9328	1.3292	0.8321
1	0	0	1	Lii and Ozisik[12]	1.4000	0.9084	0.3411
1	0	0	1	Sutton[11]	1.6279	0.8639	0.0000
1	0	0	1	Barker and Sutton[10]	1.6261	0.8643	0.0000
1	0	0	1	Present work	1.6308	0.8629	0.0001
0.5	0.5	0.5	0.5	Lii and Ozisik[12]	0.5317	0.6188	0.5884
0.5	0.5	0.5	0.5	Sutton[11]	0.9944	0.7018	0.2810
0.5	0.5	0.5	0.5	Barker and Sutton[10]	0.9938	0.7026	0.2812
0.5	0.5	0.5	0.5	Present work	0.9957	0.7002	0.2801

Table 3 Numerical experiment for $\Delta\xi$ at $\theta_1 = 1$, $\theta_2 = \theta_0 = 0$, $\omega = 0.9$, $\epsilon_1 = \epsilon_2 = 1$, $\tau_0 = 2$, and $\xi = 0.05$

	θ			$Q^r/4\pi N$		
$\Delta\xi$	$\tau/\tau_0 = 0.25$	0.50	0.75	$\tau/\tau_0 = 0.25$	0.50	0.75
			$N = 0.01$			
0.00125	0.03742	0.02614	0.01782	13.740	10.602	8.423
0.00125/2	0.02648	0.01930	0.01350	13.368	11.098	9.466
0.00125/3	0.02648	0.01930	0.01350	13.369	11.098	9.466
			$N = 0.001$			
0.00125	0.26463	0.19303	0.13505	133.704	111.058	94.735
0.00125/2	0.26456	0.19303	0.13507	133.793	111.129	94.803
0.00125/3	0.26453	0.19302	0.13507	133.816	111.161	94.833

boundary intensities, we can express

$$S_{ap}(\tau,\mu,\xi) = \frac{(\tau_{i+1}-\tau)(\mu_{j+1}-\mu)}{\Delta\tau\Delta\mu} S_{i,j} + \frac{(\tau-\tau_i)(\mu_{j+1}-\mu)}{\Delta\tau\Delta\mu} S_{i+1,j}$$
$$+ \frac{(\tau_{i+1}-\tau)(\mu-\mu_j)}{\Delta\tau\Delta\mu} S_{i,j+1} + \frac{(\tau-\tau_i)(\mu-\mu_j)}{\Delta\tau\Delta\mu} S_{i+1,j+1} \tag{9a}$$

$$i_{ap}(0,\mu,\xi) = \frac{\mu_{j+1}-\mu}{\Delta\mu} i'_j + \frac{\mu-\mu_j}{\Delta\mu} i'_{j+1} \tag{9b}$$

$$i_{ap}(\tau_0,-\mu,\xi) = \frac{\mu_{j+1}-\mu}{\Delta\mu} i''_j + \frac{\mu-\mu_j}{\Delta\mu} i''_{j+1} \tag{9c}$$

where $S_{i,j} = S(\tau_i,\mu_j,\xi)$, $i'_j = i(0,\mu_j,\xi)$, and $i''_j = i(\tau_0,-\mu_j,\xi)$ are the nodal parameters. $\Delta\tau = \tau_{i+1} - \tau_i$, and $\Delta\mu = \mu_{j+1} - \mu_j$.

Table 4 Effect of scattering anisotropy on the time to reach steady state at $\epsilon_1 = \epsilon_2 = 1$, $\omega = 0.9$, $\tau_0 = 2$, $\theta_1 = 1$, $\theta_2 = 0$, $\theta_0 = 0$, and $N = 0.001$

Phase function	Dimensionless steady-state time, ξ
$1 - \mu\mu'$	0.08375 (0.04125)
1	0.07875 (0.03875)
$1 + \mu\mu'$	0.07375 (0.03500)

Substitution of Eqs. (9) into Eqs. (4–6) constructs the expressions for approximation functions $S_{ap}(\tau,\mu,\xi)$, $i_{ap}(0,\mu,\xi)$, and $i_{ap}(\tau_0, -\mu,\xi)$. These equations, of course, hold for all values of τ and μ and, consequently, at nodal points in particular. Equations (4–6) are then replaced by a set of approximate nonhomogeneous linear algebraic equations to solve for the

Table 5 Effect of anisotropic scattering on temperatures at $\xi = 0.01$, $\theta_1 = 1$, $\theta_2 = \theta_0 = 0$, $\tau_0 = 2$, $N = 0.01$, and $\epsilon_1 = \epsilon_2 = 1$

	$\omega = 0.9$				$\omega = 0.1$			
τ/τ_0	$1-\mu\mu'$	1	$1+\mu\mu'$	Rayleigh	$1-\mu\mu'$	1	$1+\mu\mu'$	Rayleigh
0.00	1.0000	1.0000	1.0000	1.0000	1.0000	1.0000	1.0000	1.0000
0.05	0.5181	0.5167	0.5146	0.5168	0.6216	0.6206	0.6196	0.6206
0.15	0.0958	0.0948	0.0929	0.0946	0.2780	0.2778	0.2775	0.2777
0.25	0.0544	0.0542	0.0535	0.0540	0.1778	0.1785	0.1790	0.1783
0.35	0.0460	0.0466	0.0468	0.0463	0.1273	0.1284	0.1294	0.1282
0.50	0.0359	0.0372	0.0386	0.0370	0.0804	0.0817	0.0829	0.0816
0.65	0.0273	0.0291	0.0315	0.0289	0.0522	0.0534	0.0546	0.0533
0.75	0.0221	0.0242	0.0270	0.0240	0.0395	0.0406	0.0418	0.0406
0.85	0.0171	0.0194	0.0226	0.0192	0.0298	0.0308	0.0319	0.0308
0.95	0.0097	0.0114	0.0139	0.0113	0.0172	0.0179	0.0186	0.0179
1.00	0.0000	0.0000	0.0000	0.0000	0.0000	0.0000	0.0000	0.0000

Table 6 Effect of surface emissivity on the temperature and radiative heat-flux distribution at $\xi = 0.01$, $\tau_0 = 2$, $N = 0.01$, $\theta_1 = 1$, $\theta_2 = \theta_0 = 0$, and $\omega = 0.9$

						$\tau/\tau_0 = 0.25$			0.5			0.75		
ϵ_1	ρ_1^d	ρ_1^s	ϵ_2	ρ_2^d	ρ_2^s	$1-\mu\mu'$	1	$1+\mu\mu'$	$1-\mu\mu'$	1	$1+\mu\mu'$	$1-\mu\mu'$	1	$1+\mu\mu'$
								$\theta(\tau,\xi)$						
1	0	0	1	0	0	0.0544	0.0542	0.0535	0.0539	0.0372	0.0386	0.0221	0.0242	0.0270
0.5	0.5	0	0.5	0.5	0	0.0395	0.0390	0.0380	0.0280	0.0289	0.0298	0.0202	0.0220	0.0242
0.5	0	0.5	0.5	0	0.5	0.0397	0.0392	0.0383	0.0281	0.0290	0.0299	0.0202	0.0220	0.0241
								$Q^r(\tau,\xi)/4\pi N$						
1	0	0	1	0	0	9.721	11.232	13.384	7.504	8.982	11.110	6.670	7.457	9.477
0.5	0.5	0	0.5	0.5	0	6.103	6.677	7.387	4.445	5.007	5.712	3.250	3.743	4.367
0.5	0	0.5	0.5	0	0.5	6.079	6.645	7.344	4.415	4.969	5.663	3.220	3.705	4.318

unknowns $S_{i,j}$, i_j', and i_j''. Once the approximate solutions of the source function and boundary intensities are obtained by nodal approximation from the given temperature distribution, the radiation distributions are readily determined and the temperature distribution at next time step is then obtained from Eq. (1) using the Crank-Nicolson method. The computational sequence is then repeated until the steady-state solutions are obtained. In the present study, results are obtained with the slab divided into 20 elements (21 nodes) and $0 \le \mu \le 1$ uniformly divided into 5 elements (6 nodes).

The effects of anisotropic scattering, albedo ω, conduction-to-radiation parameter, and the surfaces' emissivity on the temperature distribution and radiative heat flux are investigated. To illustrate the accuracy of the numerical method presented here, results of dimensionless temperature and heat transfer are compared with the integral transform technique,[10] hybrid Galerkin,[11] and normal-mode expansion[12] for isotropic scattering and $\Delta\xi = 0.00125$. Tables 1 and 2 show the comparisons at $\xi = 0.05$, $N = 0.1$, $\tau_0 = 1.0$, and $\omega = 0.5$. It is shown that the transient temperature and net radiative flux results using the present method are in good agreement with the results of Barker and Sutton[10] and Sutton,[11] whereas a discrepancy exists between Lii and Ozisik's[12] results and the others. This discrepancy has been addressed in Ref. 10. In the following, we focus our attention on the anisotropic scattering. Although the Crank-Nicolson difference technique is unconditionally stable, there are time-step constraints to yield physically realistic solutions. A numerical experiment is carried out here to ensure the independence of the numerical results on the time step $\Delta\xi$. Table 3 presents the temperatures and radiant flux by using the time step $\Delta\xi = 0.00125$, 0.000625, and $0.00125/3$ for $\omega = 0.9$, $\tau_0 = 2$, $\epsilon_1 = \epsilon_2 = 1$, $\theta_1 = 1$, $\theta_2 = \theta_0 = 0$, and $A_1 = 1$. It is seen that at $N = 0.01$ the results of temperature are identical to at least four digits for the latter two time steps, while the derivations of temperature and radiant flux for the three time steps listed are negligible at $N = 0.001$. The time steps in the following analysis are thus chosen to be 0.0006125 for $N = 0.01$ and 0.00125 for $N = 0.001$.

The effects of the scattering albedo ω, anisotropy of scattering, and wall surface reflectivities on the medium's dimensionless heat transfer are illustrated in Tables 4–6 and in Figs. 2 and 3. Table 4 shows the effects of anisotropic scattering on the dimensionless time to reach steady state (defined as the time for the dimensionless temperatures in two successive iterations to differ within 10^{-4} at all nodes) at $\omega = 0.9$, $N = 0.001$, $\tau_0 = 2$, $\epsilon_1 = \epsilon_2 = 1$, $\theta_1 = 1$, and $\theta_2 = \theta_0 = 0$. The values in parentheses show steady-state time in accordance with Barker's definition[10] (specifically, for total heat flux to converge within 1% of the steady-state total heat-flux value). It has been noticed that the steady-state time increases with the decrease in the conduction-to-radiation parameter.[10] It is shown here that more time is required for a strongly backscattering system to reach steady state than a strongly forward-scattering one. The reason for this is that forward scattering transports more radiative heat and more combined radiative and conductive heat, as shown in Figs. 2 and 3, from the hot region to the cold region than backscattering and, thus, leads to a faster balance in energy. The increase in the radiative heat flux due to the effect of scattering anisotropy may reach up to more than 50%, whereas the difference in dimensionless temperature due to the effect of anisotropic scattering at some nodal points may reach up to more than 20% in the present study, as shown in Table 5. However, the difference between the isotropic and Rayleigh scattering is small. Table 5 also shows that a strong backscattering leads to an increase of the temperature near the hot surface and a decrease of the temperature near the cold wall. Figure 2 also shows the variation of total heat flux with respect to dimensionless time at three positions along the slab layer. Table 5 also shows the effect of albedo on the temperatures. The results show that decreasing the value of ω increases the temperature. Moreover, as expected, the effect of scattering anisotropy becomes more significant with the increase in albedo ω. Table 6 shows the effect of surface emissivity on the same. As the emissivity is increased, the effect of scattering anisotropy on the radiative heat flux becomes considerable. The difference between the results of the specular and diffuse reflections is negligible. The effects of the conduction-to-radiation parameter N on the heat transfer and temperatures are shown in Figs. 4 and 5. It is seen that the effect of N on the total heat flux and temperatures is significant. Figure 5 also indicates that small N leads to a faster temperature development.

Conclusions

The problem of simultaneous conduction and radiation through absorbing, emitting, and anisotropically scattering material has been analyzed. Numerical analysis in the present study leads to the following summaries:

1) More time is required for strong backscattering in the heat-transfer system to reach steady state than strong forward scattering.

2) The difference between the effects of specular and dif-

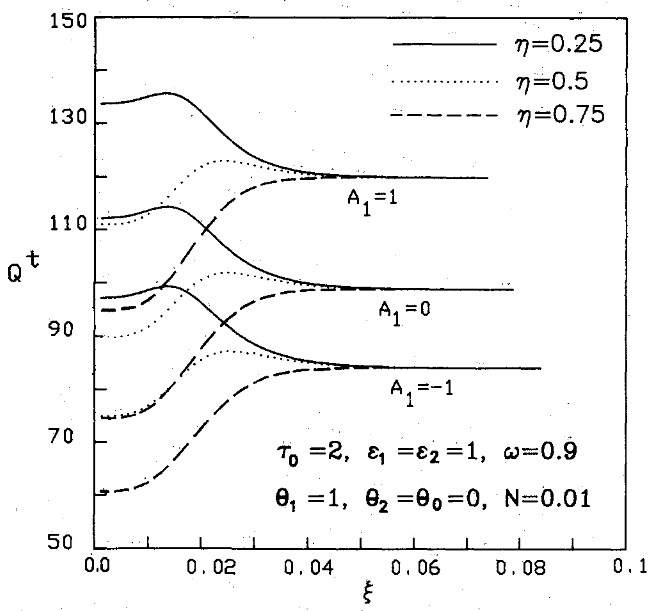

Fig. 2 Variation of the total heat flux with respect to time at three positions.

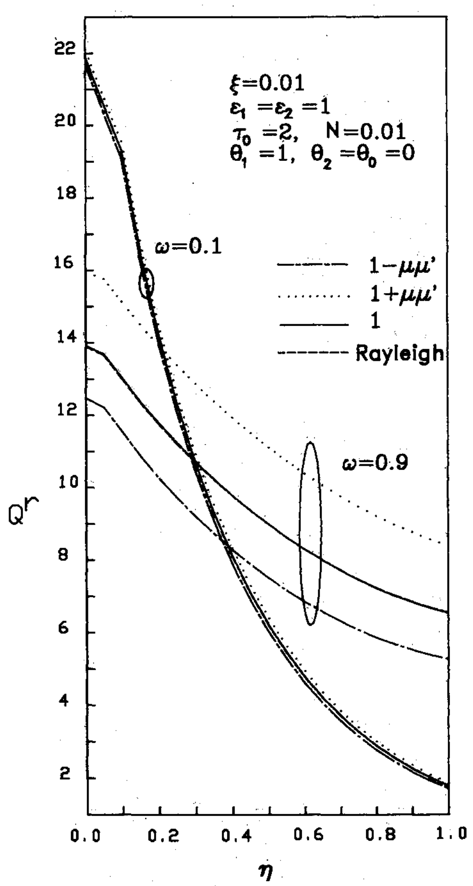

Fig. 3 Effects of anisotropic scattering and albedo on the radiant flux distribution.

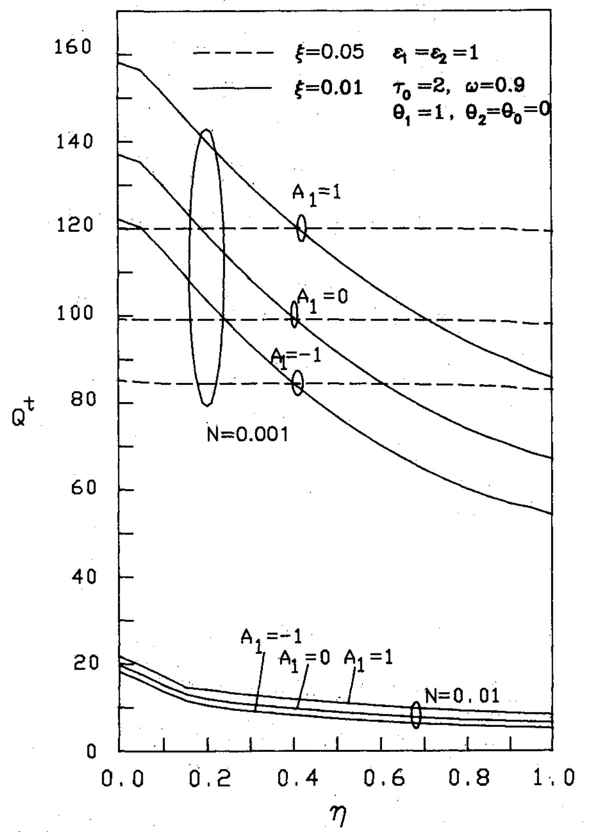

Fig. 4 Effects of N and scattering anisotropy on the total heat-flux distributions.

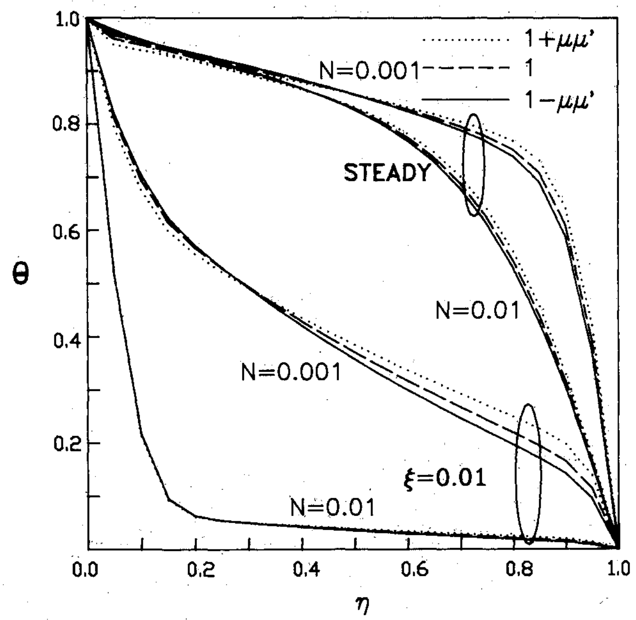

Fig. 5 Effects of N on the temperature distributions at $\epsilon_1 = \epsilon_2 = 1$, $\tau_0 = 2$, $\theta_1 = 1$, $\theta_1 = \theta_0 = 0$, and $\omega = 0.9$.

fuse reflections seems to be negligible.

3) Reflection effects at the boundary will decrease heat transfer through the medium.

4) Scattering anisotropy has an important effect on heat transfer and temperature distribution, especially for large ω.

5) The effects of conduction-to-radiation parameter, albedo ω, and surface emissivity on the temperature are significant.

References

[1]Kaviany, M., "One-Dimensional Conduction-Radiation Heat Transfer Between Parallel Surfaces Subject to Convective Boundary Conditions," *International Journal of Heat and Mass Transfer,* Vol. 28, No. 2, 1985, pp. 497–499.

[2]Yuen, W. W. and Wong, L. W., "Heat Transfer by Conduction and Radiation in a One-Dimensional Absorbing, Emitting and Anisotropically-Scattering Medium," *Journal of Heat Transfer,* Vol. 102, No. 2, 1980, pp. 303–307.

[3]Chawla, T. C. and Chan, S. H., "Solution of Radiation-Conduction Problems with the Collocation Method Using B-Splines as Approximating Functions," *International Journal of Heat and Mass Transfer,* Vol. 22, No. 12, 1979, pp. 1657–1667.

[4]Roux, J. A. and Smith, A. M., "Combined Conductive and Radiative Heat Transfer in an Absorbing Scattering Infinite Slab," *Journal of Heat Transfer,* Vol. 100, No. 1, 1978, pp. 98–104.

[5]Bergquam, J. B. and Seban, R. A., "Heat Transfer by Conduction and Radiation in Absorbing and Scattering Materials," *Journal of Heat Transfer,* Vol. 93, Ser. C, No. 2, 1971, pp. 236–239.

[6]Dayan, A. and Tien, C. L., "Heat Transfer in a Gray Planar Medium with Linear Anisotropic Scattering," *Journal of Heat Transfer,* Vol. 97, Ser. C, No. 3, 1975, pp. 391–396.

[7]Viskanta, R., "Heat Transfer by Conduction and Radiation in Absorbing and Scattering Materials," *Journal of Heat Transfer,* Vol. 87, No. 1, 1965, pp. 143–150.

[8]Viskanta, R. and Grosh, R. J., "Heat Transfer by Simultaneous Conduction and Radiation in an Absorbing Medium," *Journal of Heat Transfer,* Vol. 84, No. 1, 1962, pp. 63–72.

[9]Ratzel, A. C. and Howell, J. R., "Heat Transfer by Conduction and Radiation in One-Dimensional Planar Media Using the Differential Approximation," *Journal of Heat Transfer,* Vol. 104, No. 2, 1982, pp. 388–391.

[10]Barker, C. and Sutton, W. H., "The Transient Radiation and Conduction Heat Transfer in a Gray Participating Medium with Semi-Transparent Boundaries," *ASME Radiation Heat Transfer,* edited by B. F. Armaly and A. F. Emery, HTD-Vol. 49, 1985, pp. 25–36.

[11]Sutton, W. H., "A Short Time Solution for Coupled Conduction and Radiation in a Participating Slab Geometry," *Journal of Heat Transfer,* Vol. 108, No. 2, 1986, pp. 465–466.

[12]Lii, C. C. and Ozisik, M. N., "Transient Radiation and Conduction in an Absorbing, Emitting and Scattering Slab with Reflective Boundaries," *International Journal of Heat and Mass Transfer,* Vol. 15, No. 5, 1972, pp. 1175–1177.

[13]Tsai, J. R. and Ozisik, M. N., "Transient, Combined Conduction and Radiation in an Absorbing, Emitting and Isotropically Scattering Solid Sphere," *Journal of Quantitative Spectroscopy and Radiative Transfer,* Vol. 38, No. 4, 1987, pp. 243–251.

[14]Fernandes, R., Francis, J., and Reddy, J. N., "A Finite Element Approach to Combined Conductive and Radiative Heat Transfer in a Planar Medium," *Heat Transfer and Thermal Control,* edited by A. L. Crosbie, Vol. 78, Progress in Astronautics and Aeronautics, AIAA, Washington, DC, 1981, pp. 92–109.

[15]Hazzah, A. S. and Beck, J. V., "Unsteady Combined Conduction-Radiation Energy Transfer Using a Rigorous Differential Method," *International Journal of Heat and Mass Transfer,* Vol. 13, No. 3, 1970, pp. 517–522.

[16]Weston, K. C. and Hauth, J. L., "Unsteady, Combined Radiation and Conduction in an Absorbing, Scattering, and Emitting Medium," *Journal of Heat Transfer,* Vol. 95, Ser. C, No. 3, 1973, pp. 357–364.

[17]Tong, T. W., McElroy, D. L., and Yarbrough, D. W., "Transient Conduction and Radiation Heat Transfer in Porous Thermal Insulations," *Journal of Thermal Insulation,* Vol. 9, July 1985, pp. 13–29.

[18]Rish, J. W., III. and Roux, J. A., "Heat Transfer Analysis of Fiberglass Insulation with an without Foil Radiant Barriers," *Journal of Thermophysics and Heat Transfer,* Vol. 1, No. 1, 1987, pp. 43–49.

[19]Lin, J. D. and Tsai, J. H., "Exact Formulation of Anisotropic Scattering in an Arbitrary Enclosure," *Journal of Quantitative Spectroscopy and Radiative Transfer,* Vol. 39, No. 4, 1988, pp. 299–308.

[20]Lin, J. D., "Radiative Transfer within an Arbitrary Isotropically Scattering Medium Enclosed by Diffuse Surfaces," *Journal of Thermophysics and Heat Transfer,* Vol. 2, No. 1, 1988, pp. 68–74.

[21]Gerald, C. F. and Wheatley, P. O., *Applied Numerical Analysis,* 3rd ed., Addition-Wesley, London, 1984.